

# THERMAL QUALIFICATION OF TRANSPIRATION COOLING FOR ATMOSPHERIC ENTRY

B. Esser<sup>1</sup>, A. Gülhan<sup>1</sup>, M. Kuhn<sup>2</sup>

<sup>1</sup>DLR, Windtunnels Köln-Porz, Linder Höhe, 51170 Köln, Germany

<sup>2</sup>DLR, Inst. of Structures and Design, Pfaffenwaldring 38-40, 70569 Stuttgart, Germany

## OVERVIEW

In the arc heated facility LBK a transpiration cooling concept based on porous CMC material was qualified for application in external hypersonic flow, in particular for atmospheric entry. The experimental setup allowed a direct comparison of the thermal behaviour of transpiration cooling to a well-qualified passive thermal protection technology. Tests were performed for different coolants at various flow rates in order to identify the influence on cooling efficiency. Nitrogen, argon and helium were used as coolants. It was found that for a given configuration there is an optimal coolant flow rate for each coolant. These optimal coolant flow rates could be identified and compared for all coolants used.

## 1. INTRODUCTION

During atmospheric entry some components of a space vehicle, as e.g. nose cap, leading edges and flaps, are exposed to extreme thermal loads. These components need a sophisticated thermal protection which is commonly based on ceramic surface materials for Earth re-entry of a reusable vehicle. Ceramic materials are capable of sustaining very high temperatures. This property is used to protect the vehicle's interior from being heated, since at high surface temperature most of the huge convective heat that is generated by the hypersonic flow is radiated back to space leaving only a small fraction penetrating the surface. This passive protection philosophy, however, is limited by the surface materials' operational limit temperature. In general, these limits are exceeded for planetary entries and Earth return, but also if vehicles are designed with smaller nose radii in order to improve their flight performance. These scenarios can be met either by switching to single-serving ablative systems or by extending the capabilities of reusable systems using active cooling.

Transpiration cooling is a very promising active cooling concept. The coolant is a gas that effuses through a porous surface material to the outside without disturbing the external flow field considerably. The fundamentals of transpiration cooling were investigated since the 1950s [1, 2, 3], but applications focussed on turbine blades and combustion chambers at that time. The capabilities could significantly be extended with porous ceramic composite materials (CMC). At DLR, a transpiration cooling concept based on porous carbon reinforced carbon (C/C) was developed and successfully applied to combustion chamber cooling in rocket engines [4, 5, 6]. This concept was now adapted to atmospheric entry conditions. Its applicability as part of a thermal protection system was checked during several test campaigns in the arc heated facilities LBK.

## 2. TEST FACILITY

LBK is one of the European key facilities for qualification of thermal protection systems. Tests can be performed at realistic combinations of convective and radiative heat loads and components can be tested in an atmosphere with a realistic gas composition for time periods that are characteristic for atmospheric entry, i.e. for several minutes. A sketch of the facility with its two test legs L2K and L3K is given in Fig. 1, more details are described by Gülhan and Esser [7, 8].

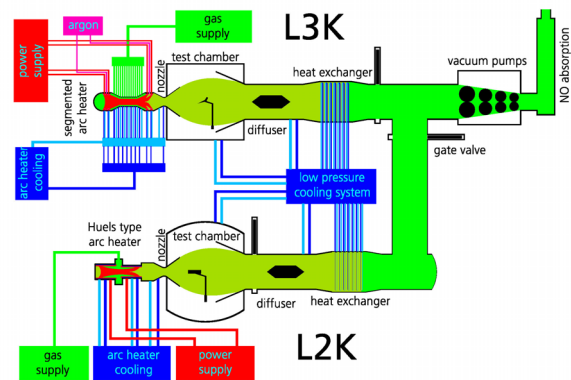


FIG 1. Sketch of the LBK facility.

Each test leg provides a hypersonic high-enthalpy flow field in the test chamber. The required energy is transferred to the working gas by an arc heater which is located upstream. At L2K, there is a Huels-type heater with an electrical power of 1 MW and at L3K a 6 MW segmented arc heater. The working gas is accelerated to hypersonic velocities by conical nozzles with a half angle of 12°. Depending on the nozzle's exit diameter Mach numbers in the range from 4 to 10 can be achieved at stagnation pressures up to 400 hPa.

Both tests legs were used for tests with transpiration cooling. First screening tests were run in the L2K facility in order to check the applicability of transpiration cooling and identify operational parameters for coolant supply [9]. For thermal qualification testing was switched to the L3K facility, where higher enthalpy levels, surface temperatures and surface pressures can be achieved.

## 3. MODEL AND INSTRUMENTATION

Thermal testing of transpiration cooled structures in a hypersonic high enthalpy flow field requires an experimental setup that allows for continuous coolant supply at

adjustable mass flow rates through a porous sample in the surface of windtunnel model. The setup that was used for the test campaign in the L3K facility is shown in Fig. 2. The complete setup is installed on top of a water-cooled model holder with a blunt nose, which is water-cooled as well. The model has an overall width of 194 mm and a length of 286 mm.

The cubic coolant reservoir which is made of C/C-SiC is mounted just on top of the model holder's base. There are three connections to the reservoir's side wall (see Fig. 2a). The left one corresponds to the coolant supply line, the other two are connectors for measuring pressure and temperature inside the reservoir. The coolant itself was supplied from K-bottles outside the test chamber with a controller installed in the supply line that allows for constant feeding at specified levels between 0.2-10 g/s. This concept had principally been approved during the screening tests. Nitrogen, helium and argon were used as coolant gases.

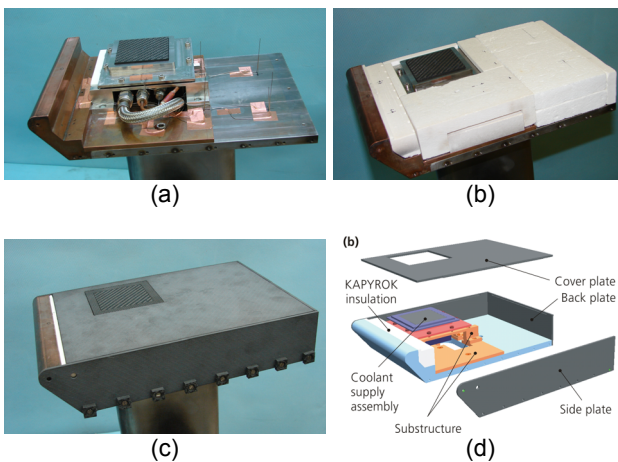


FIG 2. Setup of the test model.

For reliable operation the porous sample was installed on top of the reservoir. 61 mm wide square samples made of carbon reinforced carbon with a volumetric porosity of 17% and a thickness of 6 mm were used. A tight connection to the reservoir was obtained by a carbon seal which was compressed by a jacket frame made of high-temperature alloy PM2000.

The remaining space between the cover plate on top and the base plate was filled with insulating material as shown in Fig. 2b. The insulation prevents the aerothermal heating on the top surface from being influenced by the cooled parts of the model holder. Furthermore, the insulation material avoids internal radiation, which might lead to a substantial heating to the model's interior due to the expected high surface temperatures.

The samples are embedded in a cover plate made of carbon reinforced silicon carbide (C/C-SiC) which is a well qualified reusable high-temperature thermal protection material. Detailed information on the C/C-SiC material is given in [10, 11].

The model was primarily instrumented for temperature measurements. In total 17 thermocouples were installed inside, 8 of them were located just below the C/C-SiC

cover plate and 4 inside the insulation material. The coolant's state in the reservoir was monitored by a thermocouple and a pressure gauge. The remaining thermocouples were used to monitor the temperatures of reservoir walls, the sample's rear side and the base plate of the model holder. The locations of the thermocouples projected to the top surface are plotted in Fig. 3.

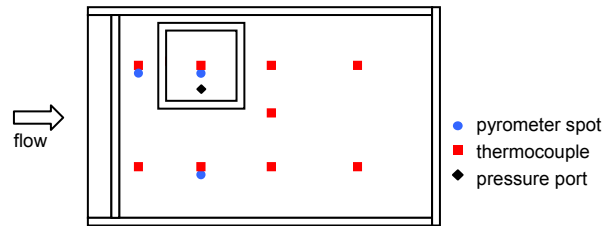


FIG 3. Locations of measurement spots.

In addition to the thermocouple measurements inside the model the surface temperature distribution was recorded by infrared cameras. During all tests a camera with a high temperature measuring range between 350°C and 2000°C was used. The temperature range was well suited for the non-cooled parts of the surface as shown in Fig. 4a. For the porous sample, however, the camera was working near to or even below the low temperature limit of its range. In order to obtain a better temperature of this particular area a second infrared camera was added which was set for measurements in the range of 0 - 500°C. The image in Fig. 4b demonstrates that the cooled parts of the surface are resolved well, while the hot parts are overexposed.

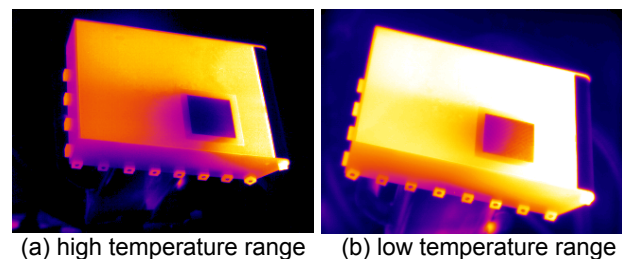


FIG 4. Typical images of the two infrared cameras (flow from right to left).

The camera measurements were supported by pyrometer measurements at specific spots on the surface, i.e. the centre of the porous sample, at the reference spot on the non-cooled side, and at a location upstream of the sample (see Fig. 3). Since the pyrometers work in the near infrared regime at about 1  $\mu\text{m}$ , their measurements are almost not affected by uncertainties in the surface material's emissivity. Therefore, they can be used to correct the results of the infrared cameras which work in the far infrared regime between 8  $\mu\text{m}$  and 13  $\mu\text{m}$  and are sensitive to emissivity. The correction procedure is described in detail by Esser et al. [12].

Due to the symmetry of the model the non-cooled side provides a kind of technological reference with regard to results of transpiration cooling, since the non-cooled surface is completely made of a reusable TPS material that is able to withstand the test conditions without being actively cooled. Therefore, the spot on the non-cooled side which

is symmetric to the centre of the porous sample can be used as reference for the measurements on the sample. The conditions are equivalent at the two locations, and the results obtained can immediately be correlated. However, it must be considered that the geometrical setup at reference spot and sample are not fully identical. The cover plate has a thickness of 3 mm and it was installed on top of insulation material, while the sample was open to the reservoir beneath and has a thickness of 6 mm.

#### 4. FLOW CONDITION AND TEST PARAMETERS

For the test campaign the L3K nozzle was set up with a throat diameter of 29 mm and an exit diameter of 300 mm. The model was placed in the free stream, 300 mm downstream of the nozzle exit. Air was used as working gas. Fig. 5 shows the Mach number distribution along the nozzle. The plot refers to a computation with the CEVCATS-N code [13] which is based on measured values of reservoir pressure and gas mass flow rate and includes non-equilibrium thermodynamics and chemistry. The flow Mach number almost uniformly increases along the nozzle axis. At model location the free stream Mach number is 7.5. In lateral direction the flow field is nearly homogeneous providing constant flow properties along the width of the model. The main flow properties at model location are listed in Table 1 together with the corresponding operating conditions of the facility. Due to the high total enthalpy level, oxygen is almost completely dissociated in the free stream. The mass fractions listed in Table 1 indicate that the free stream is mainly composed of molecular nitrogen and atomic oxygen.

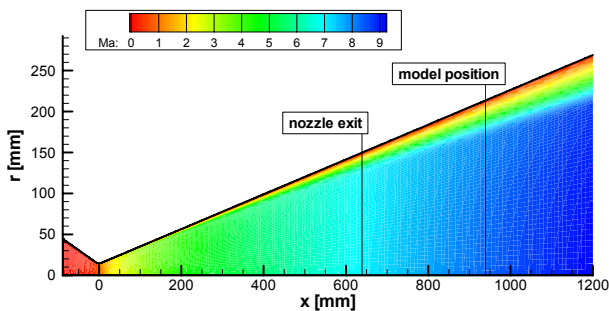


FIG 5. L3K flow field.

TAB 1. Flow conditions

reservoir pressure [hPa]	4700
reservoir temperature [K]	5650
total enthalpy [MJ/kg]	11.6
Mach number	7.5
free stream pressure [Pa]	56
free stream temperature [K]	530
free stream velocity [m/s]	3830
N <sub>2</sub> mass fraction	0.762
O <sub>2</sub> mass fraction	0.004
NO mass fraction	0.007
N mass fraction	< 10 <sup>-4</sup>
O mass fraction	0.227

The model was inclined by 20° with respect to the flow axis. All tests were performed according to the same test procedure. During facility startup the flow conditions were gradually changed until the desired operating conditions

were achieved. During this period the model was placed outside the flowfield in the background area of the test chamber in order to avoid the measurements from being influenced by changing flow conditions. In parallel, the coolant supply was started during this period as well.

As soon as the desired flow conditions were reached, and the coolant gas was being supplied at the defined mass flow rate, the test was started by moving the model to the axis of the flow field. Here, the model remained for the specified test duration which was either 180 s or 240 s. After this period, the model was moved out of the flow field, and the hypersonic flow was stopped. Data acquisition was continued for about five more minutes in order to assess additional information from the cooling phase.

#### 5. TEST RESULTS

The first tests were performed at constant coolant mass flow rate. The test matrix included variations of the coolant gas and the coolant's flow rate which besides the porous material are the main parameters for transpiration cooling in a high-enthalpy, hypersonic flow environment. The objective of the test campaign in L3K was to investigate the influence of these parameters on the local thermal behaviour of the model. In order to reduce the number of tests nitrogen was defined as baseline coolant and helium and argon were tested in comparison to nitrogen.

In a single test only one parameter combination could be tested. Proceeding that way, the facility must be able to reproduce test conditions during subsequent runs. Fig. 6 shows that the test conditions could be reproduced very well. The results of pyrometer and thermocouple measurements at the reference spot on the non-cooled side of the model are almost identical for the three tests shown. Furthermore, the good agreement proves that the results that are obtained on the non-cooled side are not influenced by the coolant flow, since the three tests were run with different nitrogen flow rates.

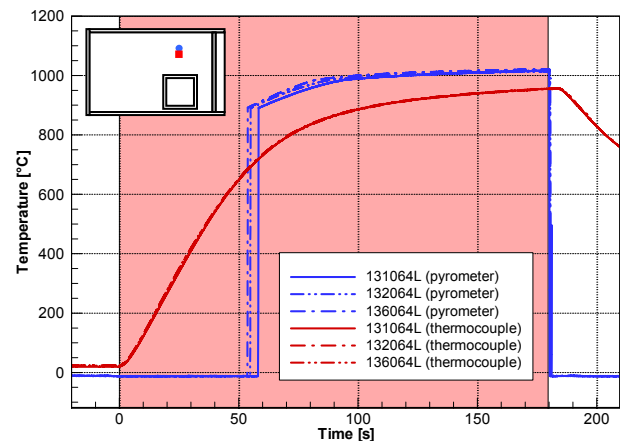


FIG 6. Pyrometer and thermocouple measurements at the reference location from three tests.

For the three tests shown the testing time was 180 s. This period is marked by a red background colour. At the end of the testing time the surface temperature which is measured by the pyrometer reaches a steady state level of

1015°C. There is a jump in the pyrometer signals about 55 seconds after the test is started. This jump is generated by the pyrometer's internal electronics. The pyrometer has a low temperature limit of 900°C, and the output signal is set artificially to 0°C as long as the measured surface temperatures are below this limit. Therefore, the signals plotted are not physical during the first 55 seconds.

The thermocouple, which is placed 3 mm below the surface just at the interface between cover plate and internal insulation, starts rising almost immediately when the model is moved into the flow field. At the end of the test it indicates a nearly constant temperature of 955°C. This value very well correlates to the measured surface temperature and the thermal properties of the C/C-SiC material.

Besides a comparison to the reference spot, valuable information on the effects of transpiration cooling are obtained from comparison to a completely non-cooled test without coolant flow. By that, influences from slightly different material and radiation properties of cover plate and sample can be excluded.

Fig. 7 shows the results of temperature measurements on the top and rear side of the porous sample during a non-cooled reference test. The temperature on the top surface which is exposed to the flow was taken from the infrared camera measurement, while the temperature on the rear surface was measured by a thermocouple.

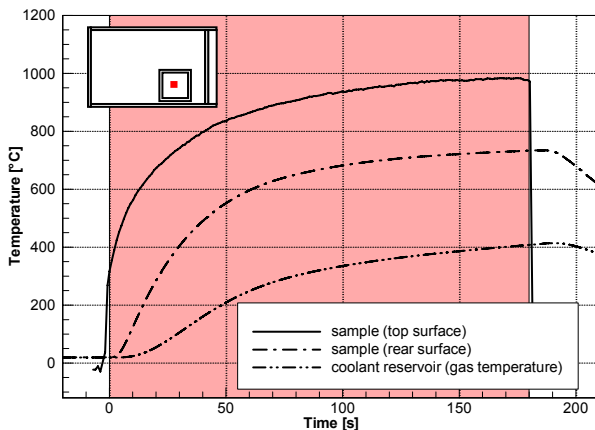


FIG 7. Temperatures measured on the sample and in the reservoir during a non-cooled reference test.

At the end of the test the top surface is heated up to 980°C, which is by 35°C lower than the temperature on the non-cooled side of the model (see Fig. 6). The difference is mainly related to different surface emissivities of the two materials. The temperature at the bottom reaches 732°C. The temperature difference between top and bottom side is significantly higher than measured for the cover plate which is mainly caused by the larger thickness of the sample. Without coolant flow the sample's porosity is not beneficial, since it allows hot gas penetrating into the reservoir. At the end of the test the temperature inside the reservoir reached 402°C, still increasing.

The infrared image in Fig. 8a shows the surface temperature distribution at the end of the non-cooled refer-

ence test. The distribution is very homogeneous, no temperature differences are observed on the cover plate in lateral direction. Only the sample and its frame show slightly different temperatures, the sample due to its different emissivity value, the frame due to a different surface coating.

Fig. 8b shows the same sample in a test with transpiration cooling, in particular nitrogen cooling at a flow rate of 0.4 g/s. The temperatures on the non-cooled side are unchanged compared to the non-cooled case. On the cooled side there are significant changes. The temperature of the sample itself is considerably reduced, and in the wake of the sample, the cover plate is cooled as well.

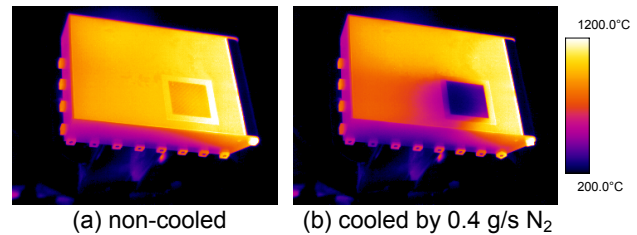


FIG 8. Infrared images taken at the end of a test without and with cooling (flow from right to left).

The sequence of infrared images in Fig. 9 shows that the differences between the cooled and non-cooled sides are even more obvious during the test. After 90 s of testing considerable differences are visible up to the downstream end of the model. Up to the end of the test this region shrinks to about a quarter of its length. In this region surface heating is delayed considerably by transpiration cooling.

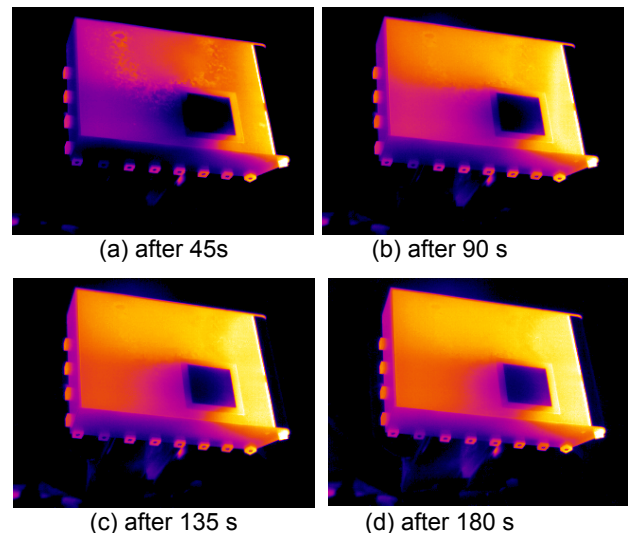


FIG 9. Sequence of infrared images in a cooled test (0.4 g/s N<sub>2</sub>).

As shown in Fig. 10 the temperature increases up to 280°C in the centre of the sample when cooling with nitrogen at 0.4 g/s. Compared to the non-cooled reference test this is a reduction by about 700°C. Although the surface temperature did not reach a steady state condition after 180 s, this reduction is quite impressive. It becomes even more impressive when considering that a small part is

caused by a gradual increase of the coolant's temperature. During the test the coolant inside the reservoir heats up by about 65 K. The corresponding heat is mainly transferred along the side walls of the reservoir. Unfortunately, heat penetration could not be avoided completely, since the reservoir had to be designed rigid with pressure-tight wall and it had to be placed close to the hot surface.

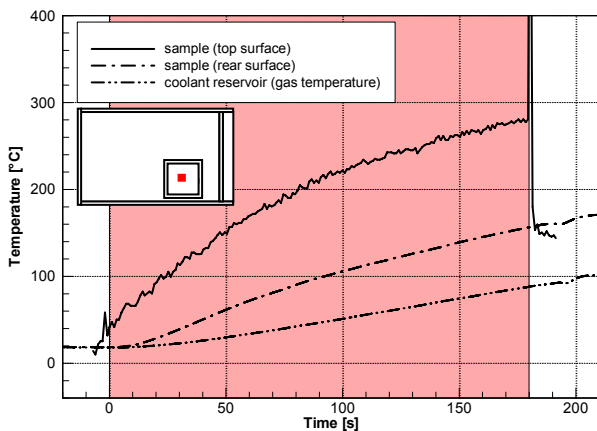


FIG 10. Temperatures measured on the sample and in the reservoir during a test with  $N_2$  cooling at a flow rate of 0.4 g/s.

When changing the coolant's flow rate the thermal response of the sample to the external heating changes as well. For nitrogen cooling the measured surface temperatures in the centre of the sample are plotted in Fig 11 for three different mass flow rates, i.e. 0.3 g/s, 0.4 g/s and 0.8 g/s, and are compared to the measurements from the non-cooled reference test.

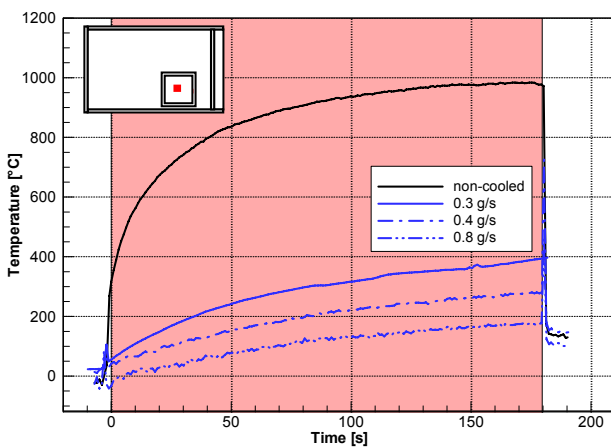


FIG 11. Surface temperatures measured in the centre of the sample for different flow rates of nitrogen.

Even for the lowest coolant flow rate of 0.3 g/s, the final temperature is remarkably reduced compared to the non-cooled test. The reduction amounts to about 500°C, from 980°C to 390°C. Increasing the flow rate to 0.4 g/s the final temperature is further reduced by another 110°C to 280°C. In order to reduce the temperature by the same amount again, the mass flow rate has to be doubled to 0.8 g/s. These values indicate that the cooling potential nonlinearly depends on the coolant's flow rate. While 0.4 g/s of

nitrogen enable a temperature reduction of 700°C, another 0.4 g/s added on top have a potential for 110°C only.

Evaluating the results with regard to space applications high coolant flow rates seem not appropriate, since a substantial amount of coolant is wasted, because it hardly contributes to a reduction of surface temperature. At very low coolant flow rates the results should be close to the non-cooled case, since the coolant cannot provide enough thermal capacity. In consequence, there should be an optimal regime in between with a considerable reduction of surface temperature at moderate coolant flow rates. Of course, this optimum depends on the heat load and on the porous material.

It was tried to assess the optimal coolant flow rate by changing the coolant flow rates during one test. Starting from a low value the coolant flow rate was gradually increased in steps and the temperature difference between the sample's rear side and the gas inside the reservoir was monitored. For nitrogen as coolant the corresponding data are plotted in Fig. 12. The test was started at a coolant flow rate of 0.4 g/s. For this value the sample's back side was heated more rapidly than the gas in the reservoir. The temperature difference increased almost linearly with time and reached 25°C after 60 seconds. Then, the coolant flow rate was increased to 0.6 g/s. The trend of the temperature difference turned from increasing to decreasing immediately. This turn was regarded to be an indication for the optimal coolant flow rate. More precisely, the last flow rate with an increasing trend was chosen to be optimal, i.e. 0.4 g/s for nitrogen.

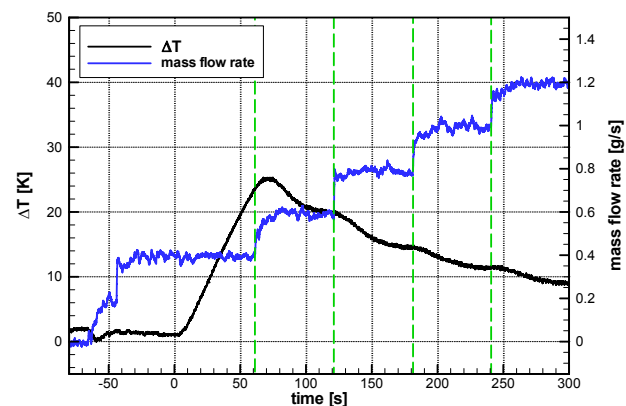


FIG 12. Temperature difference between sample and coolant measured at various nitrogen flow rates.

Corresponding dynamic tests were performed for the two other coolants, helium and argon. The optimal mass flow rates turned out to be 0.2 g/s for helium, and 0.5 g/s for argon.

At the end of the test campaign, regular tests with constant coolant flow rates were performed for the optimal flow rates. The testing time was increased to 240 seconds for these tests. The surface temperature histories that were measured in the centre of the sample are compared in Fig. 13. Since the optimal mass flow rates were found by an identical procedure, the temperature histories are similar, but there are still some differences. Although argon was supplied at a higher mass flow rate compared

to nitrogen and helium, it still provides the highest temperatures on the sample. Nitrogen is performing slightly better than helium at optimal mass flow rate, but helium has the advantage of the lowest mass flow rate.

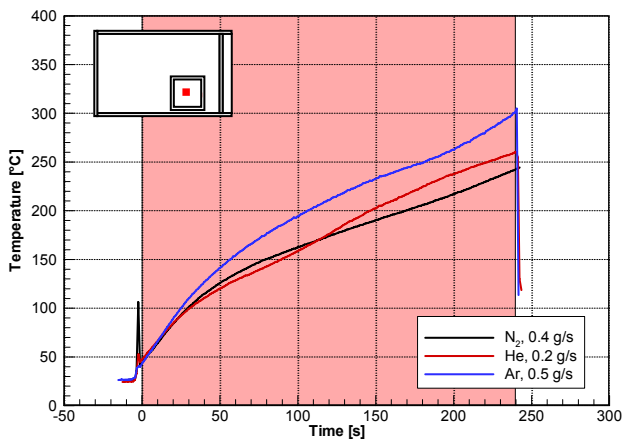


FIG 13. Surface temperatures measured in the centre of the sample for optimal flow rates of all coolants.

## 6. SUMMARY AND CONCLUSIONS

Several test campaigns were performed in the arc heated facilities L2K and L3K that qualified the concept of transpiration cooling for atmospheric entry applications. During preparatory test campaigns useful results were obtained that helped to optimize the experimental setup and the operation of coolant supply system. For the final test campaign in the L3K facility a flat plate model was used which allowed the integration of square porous samples on one side. The model setup allowed for a direct comparison of the results of transpiration cooling to a well-qualified passively cooled thermal protection technology based on C/C-SiC material.

Extensive temperature measurements were performed during the test campaign. Thermocouples were used to measure the temperature development at relevant spots inside the model. In addition, the surface temperature was observed by infrared cameras and pyrometers. The temperature measurements on the cooled samples were compared to the results of reference tests without cooling in order to quantify the influence of transpiration cooling.

From the tests at different coolant mass flow rates it was found that the efficiency of transpiration cooling nonlinearly depends on the coolant's flow rate. At very low and very high flow rates cooling is ineffective. In between there is optimum coolant flow rate. For the considered configuration with C/C samples at a model inclination of 20° the optimal flow rates were determined to 0.4 g/s for nitrogen cooling, 0.2 g/s for helium cooling and 0.5 g/s for argon cooling. The corresponding blowing ratios, which relate the coolant flow rate to the external flow rate, are 0.027 for nitrogen, 0.014 for helium and 0.034 for argon.

Accordingly, helium performs best if only the coolant's mass is taken into account. But in case of real space applications other parameters might become decisive as well. E.g., if the reservoir pressure is a limiting variable,

the optimum mass flow rates must be weighed by the coolant's molecular mass, yielding 3.96 mole/(m<sup>2</sup>s) for nitrogen, 13.9 mole/(m<sup>2</sup>s) for helium, 3.47 mole/(m<sup>2</sup>s) for argon, reversing the performance order.

## 7. REFERENCES

- [1] Rubesin, M. W., An Analytical Estimation of the Effect of Transpiration Cooling on the Heat-Transfer and Skin-Friction Characteristics of a Compressible Turbulent Boundary Layer, NACA TN 3341, Ames Aeronautical Laboratory, 1954.
- [2] Luikov, A. V., Heat and Mass Transfer with Transpiration Cooling, *Int. Journal of Heat and Mass Transfer*, 6 (1963), 559-570.
- [3] Kays, W. M., Heat Transfer to the Transpired Turbulent Boundary Layer, *Int. Journal of Heat and Mass Transfer*, 15 (1972), 1023-1044.
- [4] Lezuo, M. K., Wärmetransport in H<sub>2</sub>-transpirativ gekühlten Brennkammerkomponenten, RWTH Aachen, PhD thesis, 1998.
- [5] Serbest, E., Untersuchungen zur Anwendung der Effusionskühlung bei Raketenbrennkammern, RWTH Aachen, PhD thesis, 2002.
- [6] Ghadiani, S. R., Multiphase Continuum Mechanical Model for Design Investigations of an Effusion-Cooled Rocket Thrust Chamber, Univ. Stuttgart, PhD thesis, 2005.
- [7] Gülhan, A., Esser, B., Arc-Heated Facilities as a Tool to Study Aerothermodynamic Problems of Reentry Vehicles, in: Lu, F.K.; Marren, D.E. (Eds.): *Advanced Hypersonic Test Facilities, Progress in Astronautics and Aeronautics*, Vol. 198, p. 375-403, AIAA, 2002.
- [8] Gülhan, A., Esser, B., A Study on Heat Flux Measurements in High Enthalpy Flows, 35th AIAA Thermophysics Conference, June 11-14, Anaheim, CA, USA, AIAA 2001-3011, 2001.
- [9] Kuhn, M., Hald, H., Gülhan, A., Esser, B., Olivier, H., Experimental Investigations of Transpiration Cooled CMCs in Supersonic Plasma Flows, 5th Europ. Workshop on Thermal Protection Systems and Hot Structures, ESA-SP-631, 2006.
- [10] Hald, H., Faserkeramiken für heiße Strukturen von Wiedereintrittsfahrzeugen – Simulation, Test und Vergleich mit experimentellen Flugdaten, Institut für Bauweisen- und Konstruktionsforschung, DLR Stuttgart, PhD thesis, 2001.
- [11] Krenkel, W., Applications of Fibre Reinforced C/C-SiC Ceramics, *Ceramic Forum International* 80 (2003), No. 8, pp. E31-E38.
- [12] Esser, B., Gülhan, A., Schäfer, R., Experimental Investigation of Thermal Fluid/Structure Interaction in High Enthalpy Flow, 5<sup>th</sup> Europ. Symp. on Aerothermodynamics for Space Vehicles, Cologne, Nov. 2004, ESA SP-563, pp. 275-280, 2005.
- [13] Radespiel, R., Longo, J.M.A., Brück, S., Efficient numerical simulation of complex 3D flows with large contrast, in: 77<sup>th</sup> AGARD Fluid Dynamics Panel Meeting and Symposium on Progress and Changes in CFD Methods and Algorithms, AGARD-CP-578, 33-1, Sevilla, October 1995.